Analytical Biochemistry 430 (2012) 156–162

Contents lists available at SciVerse ScienceDirect

Analytical Biochemistry

journal homepage: www.elsevier.com/locate/yabio

An amperometric hemoglobin A1c biosensor based on immobilization of fructosyl amino acid oxidase onto zinc oxide nanoparticles–polypyrrole film

Sheetal Chawla, Chandra Shekhar Pundir *

Department of Biochemistry, Maharshi Dayanand (M.D.) University, Rohtak 124 001, India

ARTICLE INFO

Article history:
Received 7 July 2012
Received in revised form 25 July 2012
Accepted 3 August 2012
Available online 18 August 2012

Keywords:
Glycated hemoglobin
Amperometric biosensor
Fructosyl amino acid oxidase
Zinc oxide nanoparticles
Polypyrrole

ABSTRACT

Measurement of hemoglobin A1c (HbA1c, glycated hemoglobin) level in blood provides the long-term glucose level in diabetic patients without the influence of short-term fluctuations. The existing methods for HbA1c determination, including biosensors, suffer from insufficient sensitivity, detection limit, response time, and storage stability. These problems were overcome in the current biosensor. A method is described for construction of an amperometric HbA1c biosensor by immobilizing a fructosyl amino acid oxidase (FAO) onto zinc oxide nanoparticles/polypyrrole (ZnONPs/PPy) hybrid film deposited onto gold (Au) electrode and using it as working electrode, Ag/AgCl as reference electrode, and platinum (Pt) as auxiliary electrode. The whole blood samples were hemolyzed and digested by protease before measuring their HbA1c level by the biosensor. The enzyme electrode detected fructosyl valine (FV) as low as 50 μM at a signal-to-noise ratio of 3 within 2 s at +0.27 V versus Ag/AgCl, pH 7.0, and 35 °C with a linear working range of 0.1 to 3.0 mM for FV and sensitivity of 38.42 μA mM^{-1}. The electrode showed only a 30% loss of its initial response over a period of 160 days when stored at 4 °C. The biosensor measured HbA1c in whole blood of apparently healthy individuals and diabetic patients and found it to be in the ranges of 4.0% to 5.6% and 5.7% to 12.0%, respectively.

Over the past several decades, diabetes mellitus has become a major health problem worldwide, reaching epidemic proportions in many developing countries as well as in minority groups in the developed world [1,2]. Type 2 diabetes mellitus is associated with increased complications such as nephropathy, retinopathy, neuropathy, cardiovascular disease, and increased mortality. Thus, understanding the pathogenesis and preventing and ameliorating these long-term complications have been major goals of research in diabetes mellitus. Glucose reacts with the N-terminal group of the β-chain of HbA0 in blood, forming the glycated hemoglobin (hemoglobin A1c, HbA1c)[1] [3–5], and has been established as the most reliable among the various markers of glycemic control. It is also defined as the ratio between HbA1c concentration and total hemoglobin concentration. The amount of HbA1c in the erythrocytes increases with the average concentration of glucose in the blood. Because it reflects the average blood glucose level over the preceding 2 to 3 months due to the erythrocyte's life span of approximately 100 to 120 days, the determination of glycated hemoglobin is important for clinical long-term blood glucose control in individuals with diabetes mellitus [6–9]. Methods such as immunoassay, ion-exchange chromatography, boronate affinity chromatography, and electrophoresis [10–13] have been used in clinical practice to determine the glycated hemoglobin fraction. However, these suffer from certain drawbacks such as being time-consuming, labor-intensive and needing expert handling. Recently, many novel methods based on different analytical principles have been proposed, including surface plasmon resonance [14] and calorimetry [15]. However, a direct and rapid electrochemical determination of HbA1c could play a significant role in clinical analysis because it has advantages such as good selectivity, relatively low cost, and the potential for miniaturization and automation [16,17]. Hence, there is great interest to develop an electrochemical enzyme sensor for HbA1c. The enzymatic method for HbA1c assay consists of three steps: (i) proteolysis of the HbA1c β-subunits to release fructosyl amino acid (viz. fructosyl valine, FV), (ii) the oxidative deglycation of the produced FV, and (iii) the detection of the enzymatically produced hydrogen peroxide (H_2O_2). A fructosyl amino acid oxidase (FAO) catalyzes the oxidative deglycation of fructosyl amino acids to produce the corresponding amino acids, glucosone, and H_2O_2 [18] as follows:

* Corresponding author. Fax: +0 1262 274640.
E-mail address: pundircs@rediffmail.com (C.S. Pundir).

[1] *Abbreviations used:* HbA1c, hemoglobin A1c (glycated hemoglobin); FV, fructosyl valine; H_2O_2, hydrogen peroxide; FAO, fructosyl amino acid oxidase; Pt, platinum; FIA, flow injection analysis; Au, gold; ZnONP, zinc oxide nanoparticle; IEP, isoelectric point; PPy, polypyrrole; SDS, sodium dodecyl sulfate; HRP, horseradish peroxidase; $Zn(NO_3)_2{\cdot}4H_2O$, zinc nitrate; SEM, scanning electron microscopy; FTIR, Fourier transform infrared; NaOH, sodium hydroxide; EIS, electrochemical impedance spectroscopy; PBS, phosphate-buffered saline; XRD, X-ray diffraction; UV, ultraviolet.

0003-2697/$ - see front matter © 2012 Elsevier Inc. All rights reserved.
http://dx.doi.org/10.1016/j.ab.2012.08.002

$$\underset{\text{(N-terminal residue of } \beta\text{-chain in HbA1c)}}{\text{Fru-Val-His-Leu-Thr-Pro-Glu-Glu-Lys-Ser}} \xrightarrow{\text{Protease}} \underset{\text{(FV)}}{\text{Fructosyl valine}} + \underset{\text{(His,Leu,Thr)}}{(\text{amino acid})_{n-1}} \quad (1)$$

$$\text{FV} + \text{O}_2 + \text{H}_2\text{O} \xrightarrow{\text{FAO}} \text{Valine} + \text{D-glucosone} + \text{H}_2\text{O}_2 \quad (2)$$

$$\text{H}_2\text{O}_2 + 4 - \text{Amino antipyrine} \xrightarrow{\text{Peroxidase}} \text{Quinonemine dye} + 2\text{H}_2\text{O}. \quad (3)$$

So far, only a few reports have focused on the electrochemical determination of glycated hemoglobin. Tsugawa and coworkers [19] developed an enzyme sensor using a novel fructosyl amine oxidase from marine yeast. The partially purified fructosyl amine oxidase (0.05 U) was cast into a membrane and placed onto a 3-mm platinum (Pt) electrode. In addition, a dehydrogenase-based biosensor for amperometric detection of FV was reported [20], and a flow injection analysis (FIA) enzyme sensor for FV was also developed [21]. This FIA was claimed to be the first sensor toward fructosyl peptide, albeit with insufficient sensitivity. A single-use, disposable, iridium modified electrochemical biosensor was also reported [22]. However, some of these methods lead to sensors of insufficient sensitivity and repeatability. An electrochemical biosensor for FV for glycated hemoglobin detection based on core–shell magnetic bionanoparticles modified gold (Au) electrode was reported by us [23]. It had advantages of high sensitivity and a wide determining range.

Recently, the development of biocompatible nanomaterials has opened up a new direction in the development of third-generation biosensors based on direct electron transfer between enzyme and electrode. Polypyrrole is useful in construction of biosensor because of its high conductivity, good environmental stability, and large variety of applications. Special attention has been devoted to the zinc oxide nanoparticles (ZnONPs) as a surface to immobilize and modify biomolecules. Thermal stability, irradiation resistance, electrochemical activity, high electron communication features, high isoelectric point (IEP), and flexibility to form different nanostructures are the advantages that expedite its potential wide applications in biosensors [24].

The current work was aimed to construct an amperometric glycated hemoglobin biosensor based on immobilization of FAO onto ZnONPs–polypyrrole (PPy) composite electrodeposited onto Au electrode and its application for direct measurement of HbA1c in whole blood [25]. Compared with earlier amperometric biosensors, the sensor prepared by immobilizing FAO on the ZnONPs showed advantages of high sensitivity and a wide determining range.

Materials and methods

Reagents and apparatus

FAO (EC 1.5.3, 0.45 U mg^{-1} from recombinant *Escherichia coli*) was purchased from Sigma–Aldrich. CHES [2-(cyclohexylamino)ethanesulfonicacid], Triton X-100, sodium dodecyl sulfate (SDS), MES (4-morpholinoethanesulfonic acid), 4-aminoantipyrine, purified *Bacillus* sp. proteases, horseradish peroxidase (HRP), zinc nitrate [$Zn(NO_3)_2{\cdot}4H_2O$], and pyrrole were obtained from Fluka. Pyrrole was used after distillation under reduced pressure. All other chemicals were of AR (analytical reagent) grade. Fresh whole blood samples of apparently healthy individuals and diabetic patients were collected from hospital of Pt. Bhagwat Dayal Sharma (BDS) University of Health Sciences, Rohtak, India and stored at 4 °C until use.

Apparatus

All electrochemical experiments were performed on an Autolab PGSTAT 30 electrochemical workstation (Eco Chemie, The Netherlands) with GPES 4.9 software. A ZnONPs/PPy modified Au electrode of 1.0 mm diameter, a KCl-saturated Ag/AgCl electrode, and a Pt electrode served as the working, reference, and counter electrodes, respectively, and were used in all electrochemical experiments. All potentials were measured with respect to the reference electrode. Scanning electron microscopy (SEM) images were taken in a Scanning Electron Microscope (Make: Joel Japan, Model: JSM-6510), at Advanced Instrumentation Research Facility (AIRF), Jawaharlal Nehru University (JNU), New Delhi. Fourier transform infrared (FTIR) spectroscopy was performed on an FTIR spectrometer (model iS10, Thermo Electron).

Synthesis of FV

Because FV is not easily available from commercial sources, it was synthesized in our laboratory as described previously [26,27]. L-Valine (0.16 mol, 18.8 g) in 400 ml of pyridine and 400 ml of acetic acid were mixed and stirred for 30 min at room temperature. Then, 0.22 mol (40 g) of glucose (Sigma–Aldrich) was added, purged with N_2 for 5 min, and stirred for 4 days at room temperature. The dark-colored mixture was filtered, and the solvent was evaporated. A slightly yellowish amorphous product was obtained from recrystallization in methanol and lyophilized to a colorless powder.

Preparation of ZnONPs

ZnONPs were prepared according to the method described by Moghaddam and coworkers [28]. A 0.45-M aqueous solution of $Zn(NO_3)_2{\cdot}4H_2O$ and a 0.9-M aqueous solution of sodium hydroxide (NaOH) were prepared in distilled water. Then, the beaker containing NaOH solution was heated at a temperature of approximately 55 °C. The $Zn(NO_3)_2$ solution was added dropwise (slowly for 40 min) to the above heated solution under high-speed stirring. The beaker was then sealed at this condition for 2 h. The precipitated ZnONPs were finally cleaned with deionized water and ethanol and then dried in an air atmosphere at approximately 60 °C.

Preparation of ZnONPs/PPy/Au electrode

Prior to the surface modification, the Au electrode was cleaned with piranha solution (H_2SO_4/H_2O_2, 3:1, v/v) (with CARE) for 20 min and then rinsed thoroughly with distilled water. The left over piranha solution was stored in a glass bottle with vented cap for its safe disposal, as per Environmental Protection Rules. Then, the electrode was polished with alumina slurry. The electrode was successively sonicated in ethanol and distilled water to remove the adsorbed particles. First, the electropolymerization of pyrrole was carried out from pyrrole (30 mM) dissolved in $K_3Fe(CN)_6/K_4Fe(CN)_6$ electrolyte. The cycling was performed in a range of −0.2 to +0.8 V/saturated calomel electrode (SCE) at a scan rate of 20 mV s^{-1}. For electrodeposition of ZnONPs, 50 mg of ZnONPs was added in 25 ml of electrolyte [2.5 mM $K_3Fe(CN)_6/K_4Fe(CN)_6$, 1:1]. Then, PPy/ZnONPs composite was electrochemically polymerized by applying 30 polymerization cycles at −0.2 to +0.8 V at a scan rate of 20 mV s^{-1} as described previously [28]. The resulting ZnONPs/PPy/Au modified electrode was washed thoroughly with distilled water to remove unbound matter and kept in a dry Petri plate at 4 °C.

Preparation of enzyme electrode (FAO/ZnONPs/PPy/Au)

FAO was immobilized onto the ZnONPs/PPy modified Au electrode surface by physical adsorption. The high IEP of ZnONPs (9.4) makes it an excellent matrix to immobilize acidic proteins (here FAO with IEP of 4.6) by electrostatic interactions with high binding stability and insignificant protein denaturation. The biosensor was constructed by dropping 500 μl of FAO solution [by dissolving the lyophilized enzyme to a volume activity of 0.02–0.20 U/ml in potassium phosphate buffer (0.1 M, pH 7.0)] onto ZnONPs/PPy modified Au electrode surface. It was kept undisturbed for 24 h for sufficient immobilization of enzyme. The resulting enzyme electrode was dried in air and stored at 4 °C until use.

Characterization of enzyme electrode

The modification of Au electrode surface by ZnONPs/PPy and FAO was characterized by the SEM technique. The fabricated electrode (ZnONPs/PPy/Au electrode) was also characterized using FTIR spectroscopy and electrochemical impedance spectroscopy (EIS) techniques before and after immobilization of FAO. FTIR spectroscopy was performed to check the binding of FAO with ZnONPs/PPy composite film. The EIS measurements were carried out in 2.5 mM $K_3Fe(CN)_6/K_4Fe(CN)_6$ (1:1) and 0.1 M phosphate-buffered saline (PBS, pH 7.0) at ambient temperature at a polarization potential of 0.2 V in a frequency range of 0.1 to 10^4 Hz and with an amplitude of 10 mV. This study was conducted on an Autolab potentiostat/galvanostat (Eco Chemie).

Response measurement of FAO/ZnONPs/PPy/Au electrode

All electrochemical characterizations and measurements were carried out using a conventional three-electrode system with FAO/ZnONPs/PPy/Au electrode as the working electrode, a Pt wire as the auxiliary electrode, and an Ag/AgCl (saturated 3 M KCl) electrode as the reference electrode. Cyclic voltammetric measurements were carried out in a three-electrode cell containing 20 ml of electrolyte [2.5 mM $K_3Fe(CN)_6/K_4Fe(CN)_6$, 1:1], 5 ml of potassium phosphate buffer (0.1 M, pH 7.0), and 0.1 ml of FV.

Optimization of FAO/ZnONPs/Au electrode

The cyclic voltammetric peak height of the modified electrode consisting of immobilized enzyme depends strongly on the type of supporting electrolyte. Among different electrolytes tested were $K_3Fe(CN)_6/K_4Fe(CN)_6$ (2.5 mM) and KCl (1 N). To determine the optimal working conditions of the enzyme electrode, the pH of reaction buffer (0.1 M) was varied from pH 5.0 to 9.0 at an interval of 0.5 using phosphate buffer in a range of pH 5.0 to 7.0 and Tris buffer in a range of pH 7.5 to 9.0. Similarly, to determine the optimal temperature, the reaction mixture was incubated at 20 to 50 °C at intervals of 5 °C. To determine the optimal response time, the current response was studied from 5 to 25 s. To study the effect

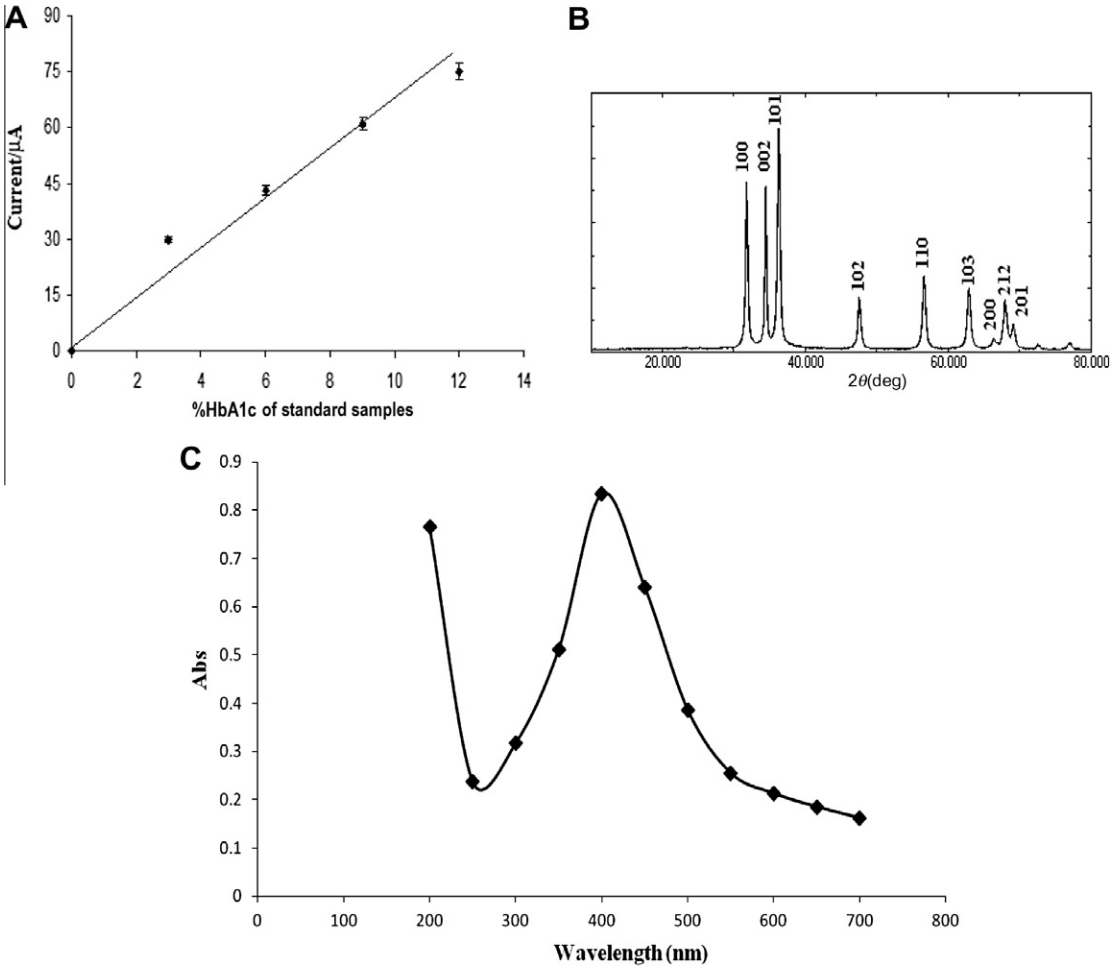

Fig.1. (A) Calibration curve between current (μA) obtained by FAO/ZnONPs/PPy/Au electrode and percentage HbA1c using standard blood samples. (B) XRD pattern of ZnONPs. (C) UV–visible absorption spectra of ZnONPs.

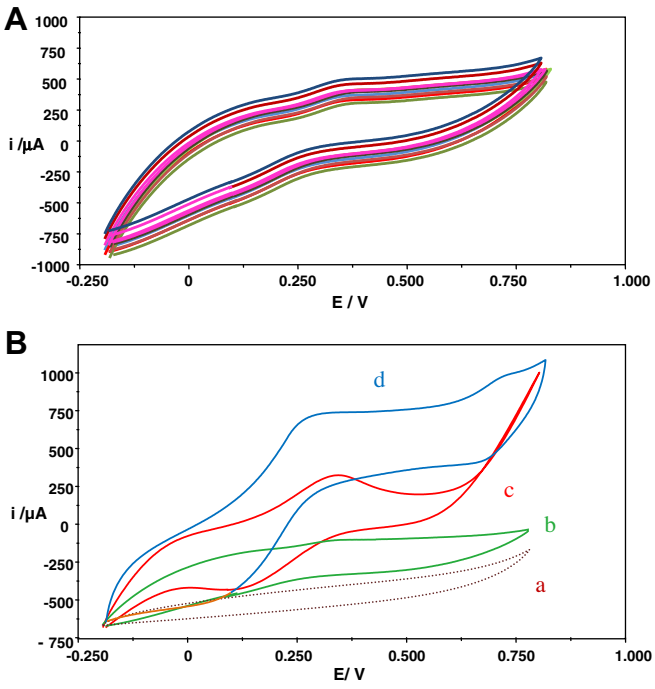

Fig.2. (A) Growth of PPy film during continuous voltammograms (10 cycles) in a solution of 30 mM pyrrole in 2.5 mM $K_3Fe(CN)_6/K_4Fe(CN)_6$ solution onto Au electrode. (B) Comparative voltammograms of bare Au electrode (curve a), PPy/Au electrode (curve b), ZnONPs/PPy/Au electrode (curve c), and FAO/ZnONPs/PPy/Au electrode (curve d) at 20 mV s^{-1}.

of substrate concentration, different FV concentrations ranging from 0.1 to 3 mM, corresponding to the physiological concentration of HbA1c [21], were used.

Detection of HbA1c in whole blood sample by FAO/ZnONPs/PPy/Au electrode

The whole blood samples of apparently healthy individuals and diabetic patients were collected with ethylenediaminetetraacetic acid (EDTA) as anticoagulant from Pt. Bhagwat Dayal Sharma (BDS) University of Health Sciences (Rohtak, India). Because HbA1c assay requires whole blood directly, no centrifugation steps were involved in separating blood cells from plasma. Prior to testing, whole blood samples were mixed by gentle inversion to resuspend settled erythrocytes. Hemolysis of the sample was performed by mixing 20 µl of whole blood with 250 µl of lysis buffer and incubated for at least 10 min at room temperature. Lysis buffer consists of 100 mM CHES (pH 8.7), 1% Triton X-100, 0.45% SDS, and 0.5 mM oxidizing agent. The lysed human whole blood samples were subjected to extensive proteolytic digestion (for 5 min) on the addition of a mixture composed of 5 mM MES (pH 7.0), 4 kU/ml purified *Bacillus* sp. Proteases, and 1 mM oxidizing agent. The proteolytic digestion led to a release of amino acids (including glycated valines from the hemoglobin β-chains), which then serve as substrates for the FAO along with another mixture composed of 0.1 M potassium phosphate buffer (pH 8.0), 90 U/ml peroxidase, and 0.8 mM 4-amino antipyrine, which cleaves N-terminal amino acid valine or histidine, resulting in production of H_2O_2 [25]. Thus, a total of 15 min time was required for the pretreatment. A calibration curve (Fig. 1A) was prepared by plotting current (µA) against different percentage of glycated hemoglobin using blood samples of known values of HbA1c (as determined by the standard immunoassay method) after giving them the above pretreatment. From this calibration curve, the value of HbA1c of unknown sample was determined. Results were evaluated using different statistical parameters and correlation with the standard immunoassay method.

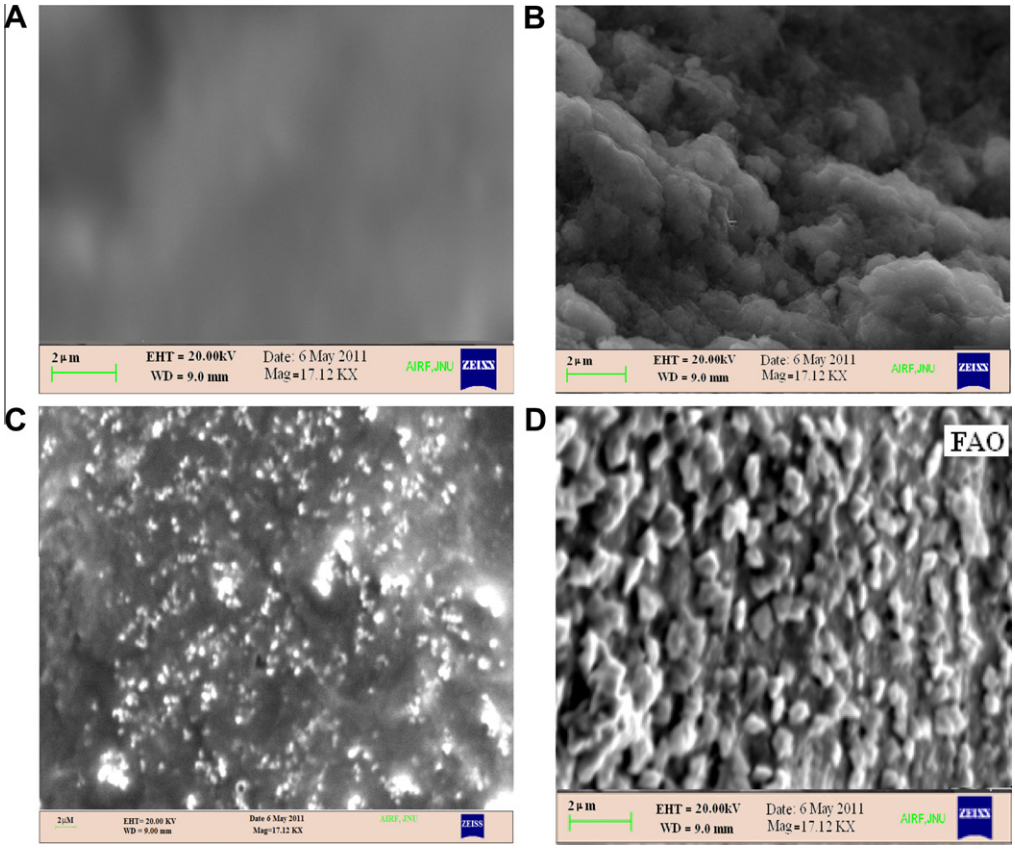

Fig.3. SEM images of bare Au electrode (A), PPy/Au electrode (B), ZnONPs/PPy/Au electrode (C), and FAO/ZnONPs/PPy/Au electrode (D).

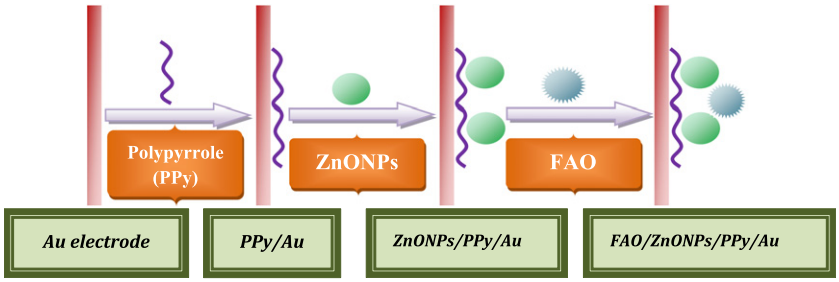

Scheme 1. Chemical sequence of electrodeposition of ZnONPs/PPy onto Au electrode and chemical reaction of immobilization of FAO onto modified Au electrode.

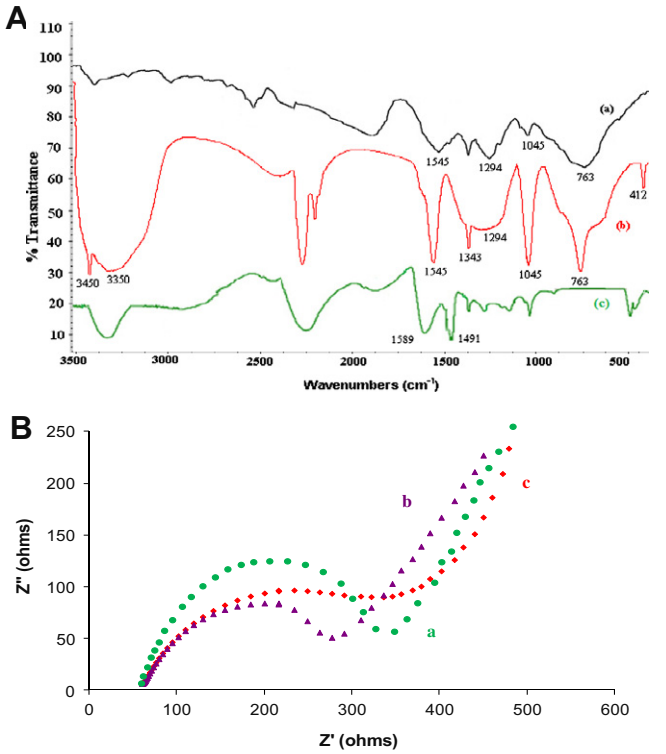

Fig.4. (A) FTIR transmission spectra of PPy/Au electrode (curve a) and ZnO/PPy/Au electrode (curve b), FAO/ZnONPs/PPy/Au electrode (curve c). (B) Nyquist plots of EIS of PPy/Au electrode (curve a), ZnONPs/PPy/Au electrode (curve b), and FAO/ZnONPs/PPy/Au electrode (curve c) in 2.5 mM $K_3Fe(CN)_6/K_4Fe(CN)_6$.

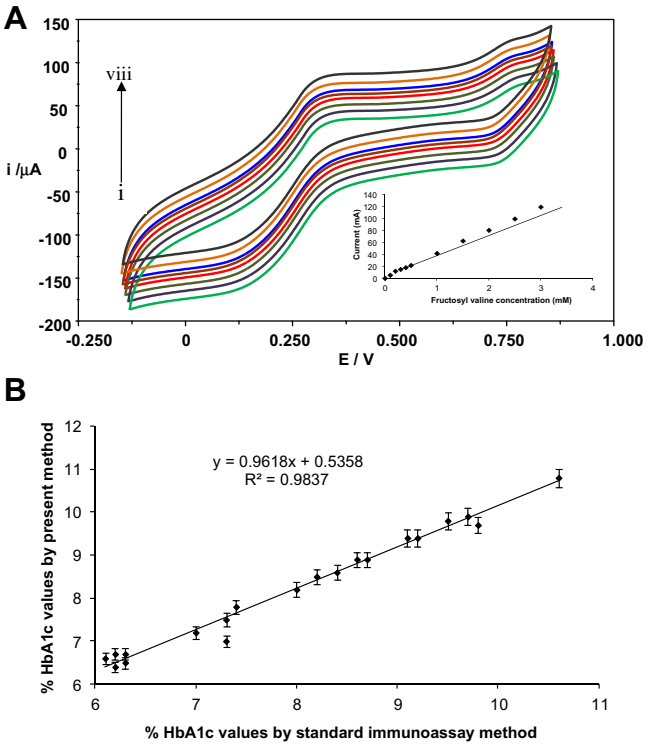

Fig.5. (A) Cyclic voltammograms recorded at different concentrations of FV from 0.1 mM (i), 0.2 mM (ii), 0.3 mM (iii), 0.4 mM (iv), 0.5 mM (v), 1 mM (vi), 1.5 mM (vii), and 3 mM (viii). Scan rate: 20 mV s^{-1} [Inset: Calibration curve for HbA1c biosensor]. (B) Correlations between percentage HbA1c values determined by standard immunoassay method (*x*-axis) and current FAO/ZnONPs/PPy modified Au electrode (*y*-axis).

Results and discussion

Characterization of ZnONPs by XRD and UV specrophotometric spectra

The fabrication of glycated Hb biosensor based on electrodeposition of ZnONPs onto Au electrode is summarized in Scheme 1. First, pyrrole was polymerized to form a PPy layer onto Au electrode by cyclic voltammetry. Then, ZnONPs were electrodeposited onto PPy/Au electrode. Finally, FAO was immobilized onto ZnONPs/PPy/Au electrode by strong electrostatic interaction. This electrode served as working electrode.

ZnONPs obtained were first characterized by X-ray diffraction (XRD) (Fig. 1B). All diffraction peaks can be indexed to hexagonal ZnO with lattice constants $a = 3.249$ Å and $c = 5.208$ Å. The characteristic peaks were higher in intensity and narrower in spectral width, indicating that the products were of good crystallinity. No peaks corresponding to impurities were detected, showing that the final products consist purely of ZnO. Characteristic peaks of ZnO at 31.8, 34.48, 36.28, and 47.5 corresponded to [100], [002], [101], and [102] diffraction peaks of the wurtzite form, indicating that the ZnONPs possessed a polycrystalline hexagonal crystal structure.

ZnONPs were also characterized by ultraviolet (UV) spectrophotometric spectra, by dispersing ZnONPs in ethanol with concentration of 0.1% wt (Fig. 1C). The spectrum reveals a characteristic absorption peak of ZnONPs at wavelength of 400 nm, which can be assigned to the intrinsic band-gap absorption of ZnO due to the electron transitions from the valence band to the conduction band (O2p → Zn3d). In addition, this sharp peak shows that the particles are in nanosize, and the particle size distribution is narrow.

Cyclic voltammetric studies

Fig. 2A shows the cyclic voltammograms recorded during 30 continuous cycles in a solution of 30 mM pyrrole in 2.5 mM $K_3Fe(CN)_6/K_4Fe(CN)_6$ solution onto Au electrode at a potential range

Table 1
HbA1c levels of apparently healthy persons, as measured by current amperometric biosensor based on FAO/ZnONPs/PPy/Au electrode.

Age (years)	Sex[a]	% HbA1c by FAO/ZnONPs/PPy/Au electrode
30	M	4.8
45	M	5.0
35	F	5.1
44	M	5.4
32	F	4.2
40	F	5.7
50	M	5.4
37	F	5.2
43	F	5.2
55	M	5.6

[a] M, male; F, female.

Table 2
HbA1c levels of diabetic patients, as measured by current amperometric biosensor based on FAO/ZnONPs/PPy/Au electrode.

Age (years)	Sex[a]	% HbA1c by FAO/ZnONPs/PPy/Au electrode
42	F	6.8
62	M	10.0
38	M	6.1
58	F	9.4
26	F	7.2
60	M	9.7
46	F	7.4
51	M	8.2
32	F	7.2
48	M	7.7

[a] F, female; M, male.

of −0.2 to +0.8 V at a scan rate of 20 mV s^{-1}, whereas Fig. 2B shows the comparative voltammograms of bare Au electrode (curve a), PPy/Au electrode (curve b), ZnONPs/PPy/Au electrode (curve c), and FAO/ZnONPs/PPy/Au electrode (curve d) at the same potential. The bare Au electrode (curve a) shows no redox peak. After 30 potential scans, only current characteristic of PPy was noticed (PPy/Au) (curve b). CV of ZnONPs/PPy/Au can be seen in curve c. Here, it can be clearly seen that the addition of ZnONPs into electrolyte solution has greatly enhanced the current with well-defined oxidation and reduction peaks of ZnONPs/PPy/Au electrode (curve c). The FAO/ZnONPs/PPy/Au exhibited a redox peak at +0.27 V (ox.), which was related to the oxidation of H_2O_2 immobilized FAO (curve d).

Electrode surface characterization by SEM and FTIR

The surface morphologies of bare electrode, PPy/Au electrode, and FAO immobilized onto ZnONPs/PPy/Au electrode were investigated using SEM (Fig. 3). The figure shows changes in surface morphology of Au electrode, as studied by SEM, after its modification by deposition of ZnONPs/PPy/Au and then immobilization of FAO onto it in chronological order. The bare Au electrode showed a uniform surface (Fig. 3A), whereas the surface of PPy modified Au electrode showed three-dimensional growth of hemispherical deposits, which generate a film of nodular morphology (commonly named "cauliflower-like" morphology) (Fig. 3B). This nodular morphology changed to uniform granular porous morphology attributed to the homogeneous dispersion of ZnONPs in PPy (Fig. 3C). The micrograph of FAO/ZnONPs/PPy/Au (Fig. 3D) clearly showed a regular globular structural morphology, indicating the successful immobilization of FAO onto the surface of modified electrode.

Fig. 4A shows the FTIR spectrum of PPy (curve a) with characteristic absorption bands at 1545 and 1343 cm^{-1} corresponding to the fundamental vibration of the pyrrole ring. The peaks at 1294, 1105, and 1045 cm^{-1} can be assigned to the =C–H in-plane vibration. The FTIR spectrum of PPy/ZnO (curve b) exhibits absorption peaks at 1545 and 1343 cm^{-1} for typical pyrrole ring vibration, and for ZnO a characteristic IR peak was observed at 412 cm^{-1}, corresponding to bending of Zn–O bond [29]. The broad peak between 3350 and 3450 cm^{-1} was due to the stretching vibrations of the –OH group on the surface of ZnONPs. FAO binding on ZnONPs/PPy/Au electrode was indicated by the appearance of additional absorption bands at 1589 and 1491 cm^{-1} (curve c), assigned to carbonyl stretch (amide I band) and–N–H bonding (amide II band), respectively.

Electrochemical impedance spectroscopy

EIS provided useful information on the impedance changes of the electrode surface during the fabrication process. The semicircular portion at higher frequencies corresponds to the electron transfer-limited process, and its diameter is equal to the electron transfer resistance that controls the electron transfer kinetics of the redox probe at the electrode interface. Meanwhile, the linear part at lower frequencies corresponds to the diffusion process [30]. Fig. 4B shows Nyquist plots of the EIS of PPy/Au electrode (curve a), ZnONPs/PPy/Au electrode (curve b), and FAO/ZnONPs/Au electrode (curve c) in 2.5 mM $K_3Fe(CN)_6/K_4Fe(CN)_6$. It can be seen that the value of resistance against charge transfer (R_{CT}) obtained as 350 Ω for PPy/Au electrode (curve a) decreased to 280 Ω for ZnONPs/PPy/Au electrode (curve b), revealing a higher electronic conducting nature of nanocomposite electrode that can be attributed to the higher surface area coupled with the conducting nature of ZnONPs, and then increased to 410 Ω for FAO/ZnONPs/PPy/Au electrode (curve c). This increase in R_{CT} could be attributed to the fact that most biological molecules, including enzymes, are poor electrical conductors at low frequency and cause hindrance to electron transfer. These results also indicate binding of FAO to ZnONPs/PPy/Au composite.

Optimization of biosensor

The experimental conditions affecting the biosensor response were studied in terms of effect of pH, incubation temperature, time, and scan rate. The optimal current was obtained within 2 s at pH 7.0 and 35 °C. The effect of the scan rate from 10 to 100 mV s^{-1} on the biosensor response using 2 mM FV in 0.1 M potassium phosphate buffer solution (pH 7.5) was also investigated. A potential scan rate of 20 mV s^{-1} was selected because with these experimental conditions the highest analytical signal and very good cyclic voltammogram profiles were obtained. The response of the current electrode system in relation to the change in FV concentration was found to be linear in the range of 0.1 to 3.0 mM.

The effect of several possible interfering substances, such as ascorbic acid, bilirubin, urea, uric acid, triglycerides, and glucose, on the current biosensor was investigated at their physiological concentration on the response of present biosensor, at 0.27 V versus Ag/AgCl in phosphate buffer (pH 7.0). Negligible interference was observed with these substances (as % decrease in biosensor response was 3.76% for bilirubin, 4.52% for triglycerides, 5.26% for urea, 8.85% for ascorbic acid, 21.28% for uric acid and 21.51% for glucose).

Evaluation of biosensor

There was a linear relationship between current and FV concentration ranging from 0.1 to 3 mM in reaction mixture (Fig. 5A), with a sensitivity of 38.42 μA mM^{-1}, which is better and higher than

that reported by Fang and coworkers (0.4 μA mM^{-1} cm^{-2}) [22]. The detection limit (S/N = 3) of the current biosensor was calculated as the lowest quantity of substrate (FV) required to give a signal to a background (blank)+3 times SD of blank and was found to be 50 μM. The limit of quantification (LOQ) of the method was 151.5 μM. To study analytical recovery, exogenous FV of known concentration was added to the whole blood sample. The concentration of HbA1c was measured in whole blood before and after the addition of exogenous FV. The percentage recovery of added FV in whole blood was calculated. The analytical recovery of added FV in whole blood (1 and 2 mM) were 94.00 to 98.90% for FAO/ZnONPs/PPy/Au electrode, indicating good efficiency of the biosensor. These values are nearly comparable to core–shell magnetic bionanoparticles modified gold electrode (95.00–98.50%) [23]. The within- and between-batch coefficients of variation for FV determination in whole blood were 1.58% and 2.07%, respectively, for FAO/ZnONPs/PPy/Au electrode, revealing the reproducibility and reliability of the method. The accuracy of the current method was tested by comparing HbA1c values (in%) in 40 whole blood samples by the current method (y) with those obtained by the standard immunoassay method (x). The values obtained by both methods showed a very good correlation ($r = 99.18$) with the regression equation $y = 0.9618x - 0.5358$ (Fig. 5B). These results indicate a very good analytical performance of the current biosensor in biological (whole blood) samples.

Determination of glycated hemoglobin in whole blood using FAO/ZnONPs/PPy modified Au electrode

HbA1c levels, as measured in human whole blood samples of apparently healthy individuals ranged from 4.0–5.7% (Table 1), which is in the normal established range. Mean HbA1c value in whole blood of diabetic patients, as measured by present biosensor was 6.5–14 %, which is highly significantly higher than those of health persons (p value <0.001) (Table 2). The elevated level of HbA1c in diabetic patients was due to comparatively higher glycation of β-chain of hemoglobin, under the prolonged increased level of blood glucose [31].

Stability and reusability of biosensor

The electrode lost 30% of its initial activity after its 260 uses when stored at 4 °C. The storage stability was 160 days for the current biosensor. The good stability and reproducibility observed for the current biosensor could be attributed to the immobilization of FAO onto ZnONPs electrodeposited onto Au electrode.

Conclusion

A novel amperometric biosensor for determination of glycated hemoglobin (HbA1c) has been fabricated, based on immobilization of FAO onto ZnONPs/PPy/Au nanocomposite. The sensor showed higher sensitivity, linearity, and stability as well as faster response time. This biosensor prototype could be used effectively as the basis for HbA1c determination for diabetic patients' medical management.

Acknowledgments

The authors are thankful to Head, Department of Biochemistry, Pt. BDS University of Health Sciences, Rohtak, for providing whole blood samples. Also, authors are thankful to head, Deptt. of Physics, Guru Jambheshwar University, Hisar (India), for providing XRD facility, for present work.

References

[1] H. King, M. Rewers, Global estimates for prevalence of diabetes mellitus and impaired glucose measurement in adults, Diabetes Care 16 (1993) 157–177.
[2] P.H. Bennett, T.A. Burch, M.A. Miller, Diabetes mellitus in American (Pima) Indians, Lancet 2 (1971) 125–128.
[3] D.E. Goldstein, R.R. Little, R.A. Lorenz, J.I. Malone, D. Nathan, C.M. Peterson, D.B. Sacks, Tests of glycemia in diabetes, Diabetes Care 27 (2004) 1761–1773.
[4] W.G. John, Haemoglobin A1c reference method, Scand. J. Clin. Lab. Invest. 66 (2006) 1–4.
[5] E.S. Kilpatrick, HbA1c measurement, J. Clin. Pathol. 57 (2004) 344–345.
[6] J.H. Ladenson, K.M. Chan, P. Kilzer, Glycated hemoglobin and diabetes: a case and an overview of the subject, Clin. Chem. 31 (1985) 1060–1067.
[7] G. Misciagna, G. Logroscino, G. De Michele, A.M. Cisternino, V. Guerra, J.L. Freudenheim, Fructosamine, glycated hemoglobin, and dietary carbohydrates, Clin. Chim. Acta 340 (2004) 139–147.
[8] F.J. Tames, J.D. Baird, A.J. Bone, $HbA1_C$ in assessment of metabolic control in diabetic BB/E rats, Diabetologia 33 (1990) 257–261.
[9] J.M. McDonald, J.E. Davis, Glycosylated hemoglobins and diabetes mellitus, Human Pathol. 10 (1979) 279–291.
[10] A.P.F. Turner, B. Chen, S.A. Piletsky, In vitro diagnostics in diabetes: meeting the challenge, Clin. Chem. 45 (1999) 1596–1601.
[11] D.E. Goldstein, R.R. Little, H.M. Wiedmeyer, J.D. England, E.M. McKenzie, Glycated hemoglobin: methodologies and clinical applications, Clin. Chem. 32 (1986) B64–B70.
[12] W.G. John, Glycated haemoglobin analysis, Ann. Clin. Biochem. 34 (1997) 17–31.
[13] J. Hageman, G. Kuehn, Assay of adenylate-cyclase by use of polyacrylamide–boronate gel columns, Anal. Biochem. 80 (1977) 547–554.
[14] J.T. Liu, L.Y. Chen, M.C. Shih, Y. Chang, W.Y. Chen, The investigation of recognition interaction between phenylboronate monolayer and glycated hemoglobin using surface plasmon resonance, Anal. Biochem. 375 (2008) 90–96.
[15] R. Rajkumar, M. Katterle, A. Warsinke, H. Möhwald, F.W. Scheller, Thermometric MIP sensor for fructosyl valine, Biosens. Bioelectron. 23 (2008) 1195–1199.
[16] G. Marko-Varga, J. Emneus, L. Gorton, T. Ruzgas, Development of enzyme-based amperometric sensors for the determination of phenolic-compounds, Trends Anal. Chem. 14 (1995) 319–328.
[17] J. Wang, Amperometric biosensors for clinical and therapeutic drug monitoring: a review, J. Pharm. Biomed. Anal. 19 (1999) 47–53.
[18] T. Horiuchi, T. Kurokawa, N. Saito, Purification and properties of fructosyl-amino acid oxidase from *Corynebacterium* sp. 2-4-1, Agric. Biol. Chem. 53 (1989) 103–110.
[19] W. Tsugawa, F. Ishimura, K. Ogawa, K. Sode, Development of an enzyme sensor utilizing a novel fructosyl amine oxidase from a marine yeast, Denki Kagaku Oyobi Kogyo Butsuri Kagaku 68 (2000) 869–871.
[20] K. Sode, F. Ishimura, W. Tsugawa, Screening and characterization of fructosyl-valine-utilizing marine microorganisms, Mar. Biotechnol. 3 (2001) 126–132.
[21] K. Ogawa, D. Stollner, F. Scheller, A. Warsinke, F. Ishimura, W. Tsugawa, S. Ferri, K. Sode, Development of a flow-injection analysis (FIA) enzyme sensor for fructosyl amine monitoring, Anal. Bioanal. Chem. 373 (2002) 211–214.
[22] L. Fang, W. Li, Y. Zhou, C.C. Liu, A single-use, disposable iridium-modified electrochemical biosensor for fructosyl valine for the glycosylated hemoglobin detection, Sens. Actuators B 137 (2009) 235–238.
[23] S. Chawla, C.S. Pundir, An electrochemical biosensor for fructosyl valine for glycated hemoglobin detection based on core–shell magnetic bionanoparticles modified gold electrode, Biosens. Bioelectron. 26 (2011) 3438–3443.
[24] E. Topoglidis, A.E.G. Cass, B. Oregan, J.R. Durrant, Immobilisation and bioelectrochemistry of proteins on nanoporous TiO_2 and ZnO films, J. Electroanal. Chem. 517 (2001) 20–27.
[25] L. Liu, S. Hood, Y. Wang, R. Bezverkov, C. Dou, A. Datta, C. Yuan, Direct enzymatic assay for% HbA1c in human whole blood samples, Clin. Biochem. 41 (2008) 576–583.
[26] P. Keil, H.B. Mortensen, C. Christophersen, A simple model of the N-terminal residue of human haemoglobin A1c, Acta Chem. Scand. B 39 (1985) 191–193.
[27] R. Rajkumar, A. Warsinke, H. Mohwald, F.W. Scheller, M. Katterle, Development of fructosyl valine binding polymers by covalent imprinting, Biosens. Bioelectron. 22 (2007) 3318–3325.
[28] A.B. Moghaddam, T. Nazari, J. Badraghi, M. Kazemzad, Synthesis of ZnO nanoparticles and electrodeposition of polypyrrole/ZnO nanocomposite film, Int. J. Electrochem. Sci. 4 (2009) 247–257.
[29] S.G. Motke, S.P. Yawale, S.S. Yawale, Infrared spectra of zinc doped lead borate glasses, Bull. Mat. Sci. 25 (2002) 75–78.
[30] Y.Q. Miao, S.N. Tan, Amperometric hydrogen peroxide biosensor based on immobilization of peroxidase in chitosan matrix crosslinked with glutaraldehyde, Analyst 125 (2000) 1591–1594.
[31] W. Azim, M. Omair, M.Q. Alam Khan, N. Shaheen, S. Azim, Correlation between glycated haemoglobin and random plasma glucose levels for the screening of diabetes mellitus, Int. J. Path. 8 (2010) 59–62.